IOP Conference Series: Materials Science and Engineering

PAPER • **OPEN ACCESS**

LTE Wide Band Metamaterial Antenna

To cite this article: M.A.M.K. Ezzat *et al* 2019 *IOP Conf. Ser.: Mater. Sci. Eng.* **610** 012085

IOP Conf. Series: Materials Science and Engineering **610** (2019) 012085 doi:10.1088/1757-899X/610/1/012085

LTE Wide Band Metamaterial Antenna

M.A.M.K. Ezzat[1], Prof.Dr. Eng.A.M. Allam[2] Dr. Eng.D.E. Fawzy[3]

Information Engineering and Technology, German University in Cairo, Cairo, Egypt[1,2]

Faculty of Engineering, Izmir University of Economics, 35330 Izmir, Turkey[3]

mostafa.kamal-ezzat@student.guc.edu.eg [1] abdelmegid.allam@guc.edu.eg [2] diaa.gadelmavla@ieu.edu.tr [3]

Abstract. This paper presents the effect of Metamaterials (MTMs) unit cells on the performance of LTE wide band antenna. It is a conventional rectangular patch antenna with dimension of 10 mm x 6 mm. It is implemented on FR-4 lossy substrate material with relative permittivity of εr = 4.4, thickness of 1.6 mm and loss tangent of 0.025. It is feed through a microstrip line with dimension of 22 mm x 3 mm. The overall dimension of the antenna is 35 mm x 35 mm x 1.6 mm. It operates over a frequency band from 2.1914 GHz to 2.6802 GHz with central frequency 2.4392 GHz and 4.831 GHz to 5.5642 GHz with central frequency 5.1573 GHz. The simulated gain at frequency 5.1573 is 3.834 dBi. MTMs cells are supporting the truncated ground layer as it widens the band and increases the gain. The antenna ground layer is replaced with different unit cell configurations, truncated ground with different array of patches, truncated ground with array of Ring Resonator (RR), truncated ground with different array of patches with vias, truncated ground with array of RR with vias, and truncated mushroom grounded. The antenna is supported with MTMs conducts gain 5.6 dBi. The design is implemented through CST microwave studio and measured through network analyzer.

1. Introduction

Long Term Evolution (LTE) is the next-generation 4G technology for both Global System for Mobile communication (GSM) and Code Division Multiple Access (CDMA) cellular carriers. It has a download rate of up to 173 Mb/sec. It uses wideband for higher data rate. LTE has a latency of Idle to active less than 100ms. LTE can stream videos and live videos. No packet switching. All packet switched data (voice and data) [1-5].

MTMs are intermittent structures that depend on LCR resonators, with the degree of inductance, capacitance and resistance required of electromagnetic resonators. MTMs are non-conventional materials. They are not found in nature. Its' properties are gained from its microstructure of unit cells not from chemical properties. They exhibit negative permittivity and permeability. These properties have a negative index of refraction till a zero index of refraction.

Linear MTM structures have been used to create these and other devices. Nonlinear MTMs are used in demonstrating phase conjugation, harmonic generation, mixing, and shifting of a resonant frequency [6-10].

In this paper, a microstrip feed patch antenna is designed to conduct a wider for LTE application at 2.4 GHz and 5GHz. The effect of different MTM cells is presented.

2. Antenna Design

2.1. Design

Figure 1 shows the conventional LTE wideband antenna. It is composed of one rectangle patch implemented on FR-4 lossy substrate with relative permittivity of εr = 4.4 and thickness of 1.6 mm. The overall dimension of the antenna is 35 mm x 35 mm x 1.6 mm. The main parameters of the proposed antenna is depicted in table 1. The feeding line dimension is 22 mm x 3 mm. The ground is truncated with the dimension of 21 mm x 35 mm as shown on Fig. 1b.

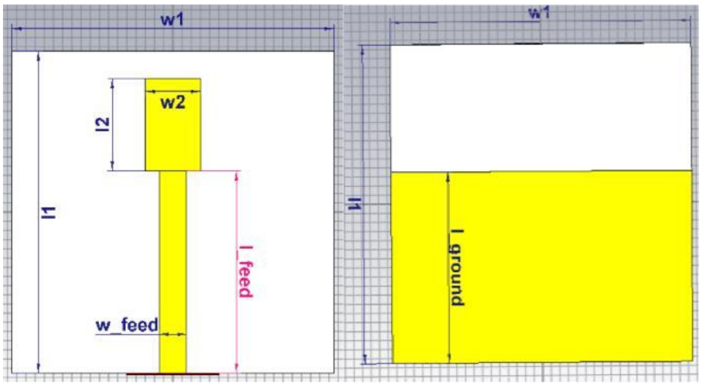

(a) (b)

Figure 1 Conventional LTE wideband antenna.
a) Top view b) Bottom view

Table 1 Dimensions of figure 1

Notations	Values/mm
W1	35
L1	35
W2	6
L2	10
L_feed	22
W_feed	3
L_ground	21

Figure 2 depicts the truncated ground with 4x4 array with different unit cell configurations, truncated ground with different array of patches (figure 2a), truncated ground with array of RR; (figure 2b), truncated ground with different array of patches with vias (figure 2c), truncated ground with array of RR with vias (figure 2d), and truncated mushroom grounded. The vias in figure 3c and figure 3d with dimensions depicted in table 2 are inserted from the middle of each patch through the substrate.

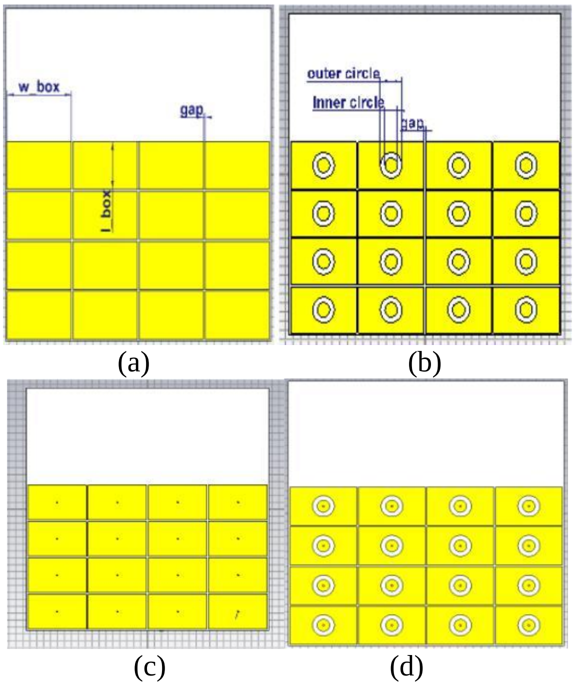

Figure 2 Different structures of the truncated grounds

a) Patches b) Patches with RR

c) Patches with Vias d) Patches with RR and Vias

Table 2 Dimensions of figure 2

Notations	Values/mm
W_box	8.5
L_box	5.05
Gap	0.2
Inner circle	0.8
Outer circle	0.8

Moreover, another configuration is illustrated in figure 3 which represents mushroom ground for the same antenna. The original truncated ground is covered with additional FR-4 substrate layer supported by another truncated ground of array of patches connected to the original ground through vias as shown as figure 3b.

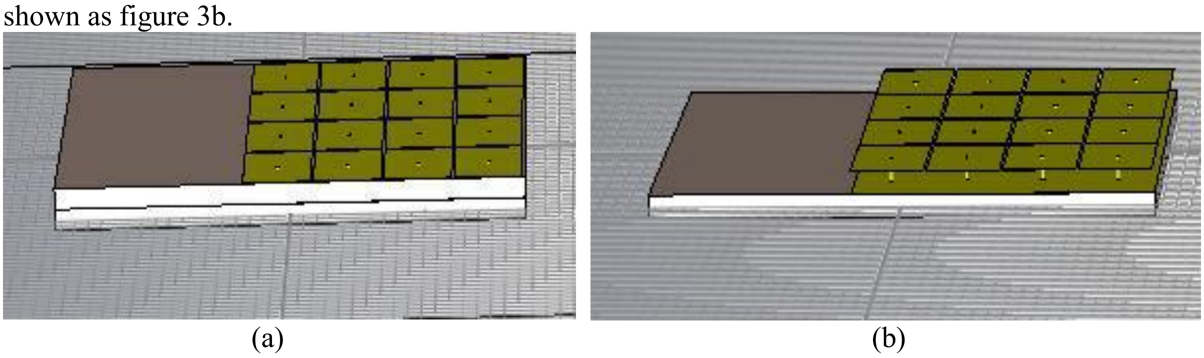

Figure 3 Mushroom Ground (a)Truncated Ground Structure No Additional Substrate, (b)Additional Substrate Added

2.2. Results

Concerning the antenna with truncated ground of array of patches (Fig. 2a), the simulated return loss is illustrated in Fig. 4 for different array sizes (4x4, 5x5, 6x6, 7x7). One notices that the antennas operate on the bands from 2.1914 GHz to 3.6802 GHz and 4.831 GHz to 5.5642 GHz which conducts LTE applications. For 6x6 array the gain is 3.834 dBi at central frequency 5.1573 GHz.

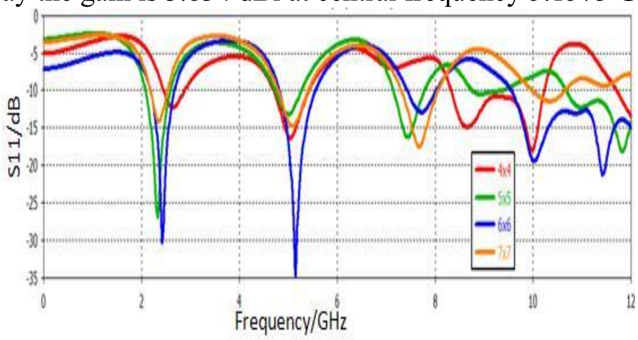

Figure 4 Return Loss of Different Number of Patches of Figure 3a

For the truncated ground with array of RR (figure 2b) the return loss is depicted in figure 5. It's clear that again the antenna resonant at different frequency bands with different number of arrays (4x4, 5x5, 6x6, 7x7). One sees that the antennas operate over the band (2.1752 GHz to 2.633 GHz) and (4.774 GHz to 5.5405 GHz). The case of (6x6) has a central frequency 2.4265 GHz and 5.1274 GHz. The gain at frequency 5.1274 GHz is 3.803 dBi.

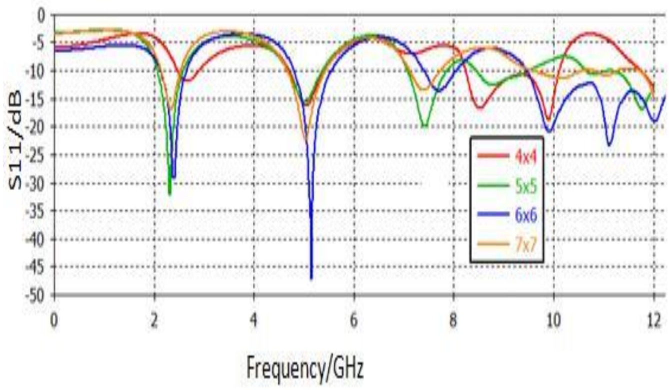

Figure 5 Return loss of different number of patches of Figure 3b

Moreover, when vias are added to the truncated ground of array of patches the return loss conducts the frequency bands depicted in figure 6 for different array size (4x4, 5x5, 6x6, 7x7). The antennas operate on the band between (2.208 GHz to 2.676 GHz) and (4.824 GHz to 5.532 GHz). In case of (6x6) it has central frequency of 2.436 GHz and 5.148 GHz. The gain at frequency 5.1573 GHz is 3.83 dBi. Changing of number of array elements will change the number of operating bands.

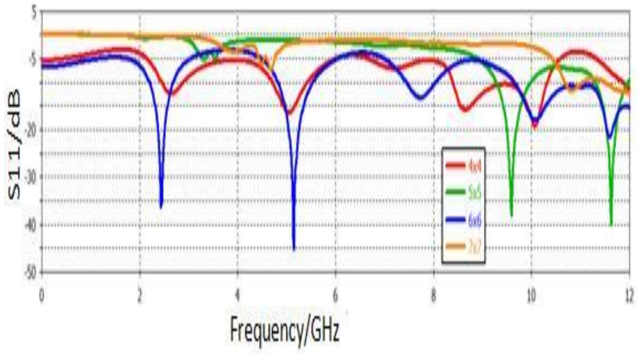

Figure 6 Return loss of different number of patches of Figure 3c

However, when the truncated ground is replaced with array of RRs and vias with different sizes (4x4, 5x5, 6x6, 7x7), the return loss conducts frequency band; 2.088 GHz to 2.568 GHz. The case of (5x5) has a central frequency 2.316. The gain at frequency 2.316 GHz is 2.32 dBi. Changing of number of array elements will change the number of operating bands.

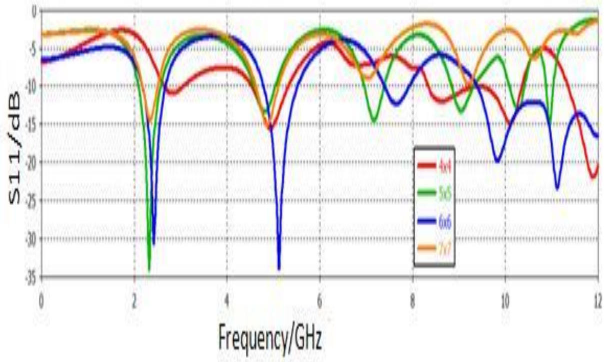

Figure 7 Return loss of different number of patches of figure 3d

Furthermore, when one used mushroom ground, the return loss shows different bands of LTE bands from 3.5668 GHz to 3.6499 GHz and 4.9555 GHz to 5.196 GHz as depicted in figure 9. The gain at frequency 3.6024 GHz is 3.174 dBi.

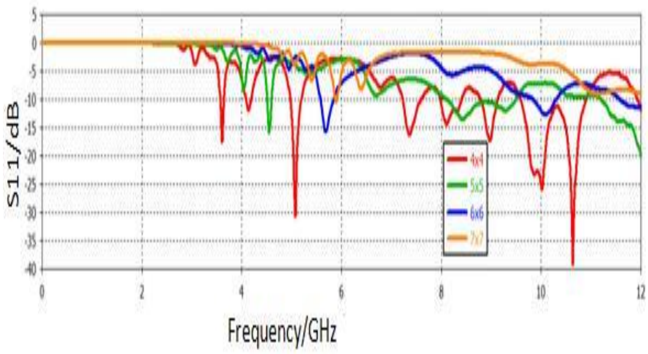

Figure 8 Return Loss of Different Number of Patches of Fig. 4b

For the sake of measurements 6x6 array of patches is fabricated as shown in Figure 9 and measured using both network analyzer and anechoic chamber. The antenna dimensions are depicted in table 3. The simulated and measured return loss are illustrated in figure 10. The radiation pattern is shown in figure 11. The fabricated antenna is shown in figure 12. The simulated gain versus frequency is presented in figure 13, where the measured gain at frequency 2.19 GHz and 2.4 GHz are 2.3 and 2.4

respectively which are quiet matched with the simulated results. The surface current is illustrated in the following figure 14. It shows that the current is accurately outlined on the antenna edges.

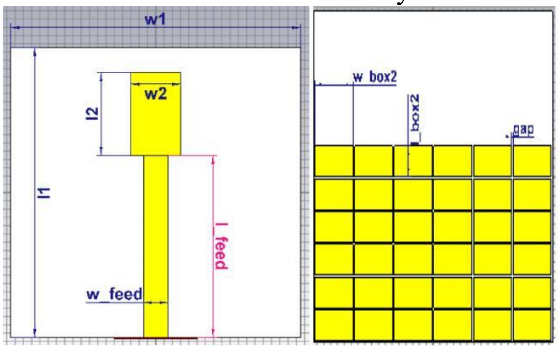

Figure 9 Top and Bottom View of the 6x6 Array of Patches Designed on CST.

Table 3 The Missing Dimensions of figure 9

Notations	**Values/mm**
W_box2	5.6
L_box2	3.26
Gap	0.2

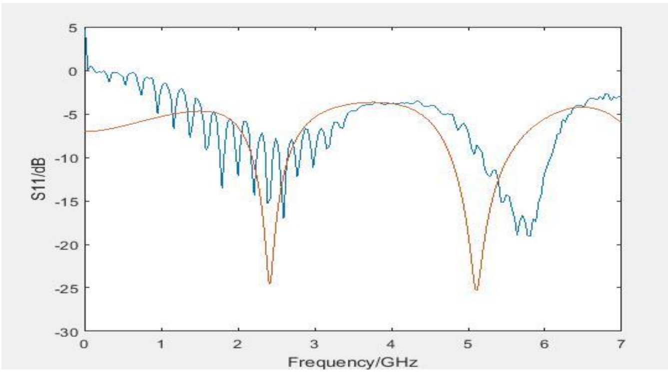

Figure 10 The Simulated and Measured Return Loss

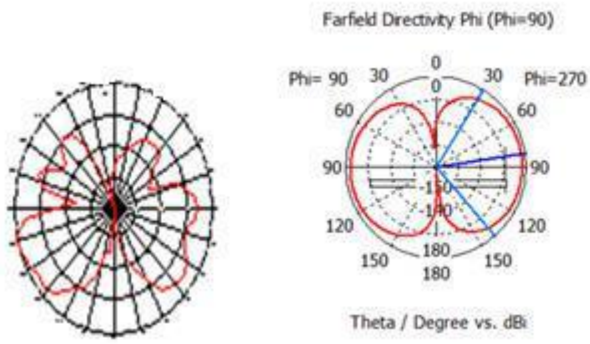

(a) Measured (b) Simulated

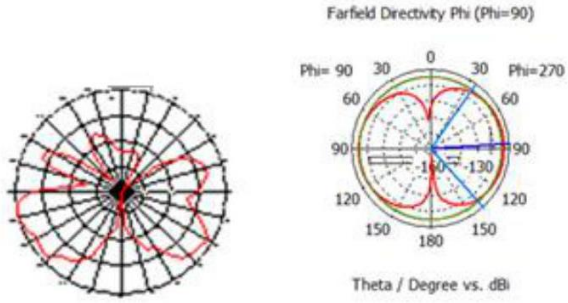

(c) Measured (d) Simulated

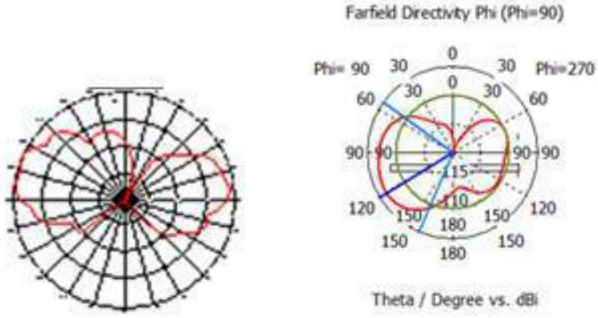

(e) Measured (f) Simulated

Figure 11 Radiation Pattern
(a) & (b) are at frequency 2.19 GHz
(c) & (d) are at frequency 2.40 GHz
(e) & (f) are at frequency 5.12 GHz

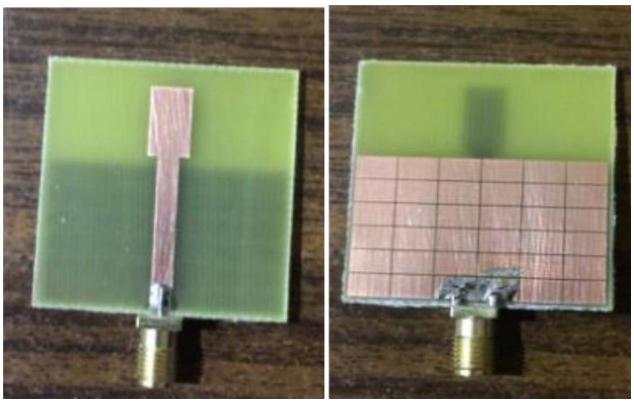

(a) (b)

Figure 12 Fabricated Antenna
a) Top View b) Bottom View

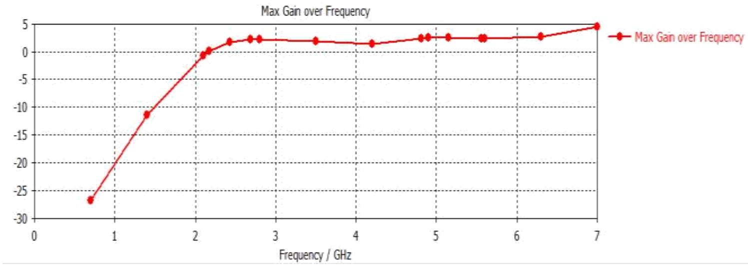

Figure 13 Maximum Over Gain Graph

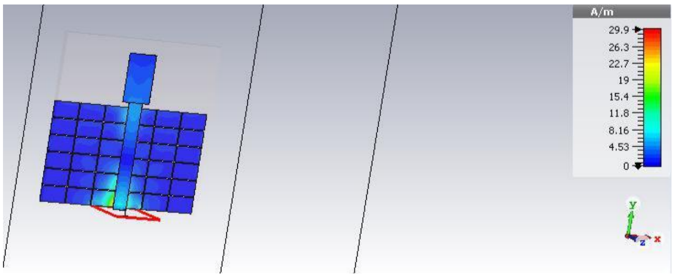

Figure 14 Surface Current at Frequency 2.4 GHz

3. Conclusion

This paper illustrates the design, analysis and implementation of LTE wide band antenna. The paper contains 5 different configurations of truncated ground. It is simulated using CST. It is fabricated on FR-4 and measured using both network analyzer and anechoic chamber. It conducts different LTE application bands. There is a good agreement between the simulated and measured results. The use of different shapes of MTMs enhances the gain. The RR are important to study as it widens the band. I highly recommend the use of them in further researchers.

References

[1] H. Ekström, A. Furuskär, J. Karlsson, M. Meyer, S. Parkvall, J. Torsner, and M. Wahlqvis t, "Technical Solutions for the 3G Long-Term Evolution," IEEE Commun. Mag., vol. 44, no. 3, March 2006, pp. 38–45.

[2] 3rd Generation Partnership Project (3GPP); Technical Specification Group Radio Access Network; Physical Layer Aspects for Evolved UTRA, http://www.3gpp.org/ftp/Specs/html-info/25814.htm.

[3] M. Danis h Nis ar, Hans Nottensteiner, and Thomas Hindelang, "On Performance Limits of DFT-Spread OFDM Systems", in Sixteenth IS T Mobile Summit, July 2007 in Budapest, Hungary.

[4] B.E. Priyanto, H. Codina, S. Rene, T.B. Sorensen, P. Mogensen, "Initial Performance Evaluation of DFT-Spread OFDM Based SC-FDMA for UTRA LTE Uplink", IEEE Vehicular Technology Conference (VTC) 2007 Spring, Dublin, Ireland, Apr. 2007.

[5] Hyung G. Myung, Junsung Lim, and David J. Goodman, "Single Carrier FDMA for Uplink Wireless Transmis sion", IEEE Vehicular Technology Magazine, vol. 1, no. 3, Sep. 2006, pp. 30–38.

IOP Conf. Series: Materials Science and Engineering **610** (2019) 012085 doi:10.1088/1757-899X/610/1/012085

[6] D. Schurig, J. J. Mock, B. J. Justice, S. A. Cummer, J. B. Pendry, A. F. Starr, and D. R. Smith, "Metamaterial electromagnetic cloak at microwave frequencies," Science, vol. 314, no. 5801, pp. 977–980, 2006.
[7] N. Landy, S. Sajuyigbe, J. J. Mock, D. R. Smith, and W. J. Padilla, "Perfect metamaterial absorber," Phys. Rev. Lett., vol. 100, p. 207402, 2008.

[8] S. Gu, J. P. Barrett, T. H. Hand, B.-I. Popa, and S. A. Cummer, "A broadband low-reflection metamaterial absorber," J. Appl. Phys., vol. 108, p. 064913, 2010.

[9] I. V. Shadrivov, S. K. Morrison, and Y. S. Kivshar, "Tunable split-ring resonators for nonlinear negative-index metamaterials," Opt. Exp., vol. 14, no. 20, pp. 9344–9349, 2006.

[10] D. Huang, E. Poutrina, and D. R. Smith, "Analysis of the power dependent tuning of a varactor-loaded metamaterial at microwave frequencies," Appl. Phys. Lett., vol. 96, no. 10, p. 104104, 2010.